Surface and Bulk Charge Density Wave Structure in 1T-TaS_2

B. Burk,* R. E. Thomson, John Clarke, A. Zettl

Incommensurate charge density waves (CDWs) in some materials form domains within which the CDWs may be commensurate. However, two questions have remained controversial: What is the geometrical structure of these domains, and are they or are they not identical on the surface and in the bulk? To address these issues in the triclinic (T) phase of tantalum disulfide (1T-TaS_2) the CDW domain structure has been accurately determined for both the crystal surface and the crystal bulk. By analyzing the bulk CDW wave vectors and associated satellites by x-ray diffraction, it is found that the bulk contains three dimensionally ordered striped domains that have previously been misidentified. Scanning tunneling microscope images show that the striped domain configuration propagates unaltered to the crystal surface, and their Fourier transforms yield the same satellite positions as the x-rays. These observations demonstrate that the surface and bulk CDW domain structures in 1T-TaS_2 are identical.

Many low-dimensional metals undergo a phase transition to a CDW state in which the conduction electron density and atomic positions become periodically modulated. The CDW quantum state is a collective mode exhibiting unique structural, electrodynamic, and thermodynamic properties that are fundamentally different from those of normal metals. The quasi–two-dimensional material 1T-TaS_2 displays a rich variety of CDW phases (*1*–*3*). At low temperatures ($T < 183$ K) the CDW modulation is commensuarate with the underlying lattice, but at higher temperatures the CDW wave vectors deviate slightly from the commensurate value. A topic that has received a great deal of experimental and theoretical attention is the possible existence of CDW domains, where the globally incommensurate CDW is drawn locally into commensurate regions; these regions or domains may be periodically ordered and separated by well-defined phase slips.

From their x-ray and theoretical studies of the nearly commensurate (NC) phase of 1T-TaS_2 (obtained between 353 and 183 K upon sample cooling), Nakanishi, Shiba, and co-workers (*4*, *5*) deduced a domain structure for which CDW phase and amplitude are modulated in a hexagonal pattern; recently these domains have been observed experimentally on the crystal surface by scanning tunneling microscopy (STM) studies (*6*–*8*). In the triclinic (T) phase of 1T-TaS_2 (obtained between 223 and 283 K upon sample warming), a related domain structure has been predicted by Nakanishi and Shiba (*9*). The model for the T phase is based on x-ray diffraction work by Tanda and Sambongi (*3*, *10*), who attempted a precise measurement of the CDW wave vectors from which they inferred a "stretched honeycomb" domain structure.

In an STM study of the CDW phases of 1T-TaS_2, Thomson *et al.* (*11*) found evidence for domains in the T phase. However, careful scrutiny of the STM images shows that the apparent domains are not entirely consistent with the generally accepted stretched honeycomb model. This discrepancy suggests that the surface CDW structure (probed by STM) and the bulk CDW structure (probed by x-ray diffraction) are significantly different in 1T-TaS_2 (and perhaps in other CDW materials as well). To investigate this interesting possibility, we performed detailed STM and x-ray diffraction studies of the T phase. In both experiments we obtained satellite structure consistent with a striped domain configuration, rather than the previously accepted stretched honeycomb configuration. In the crystal bulk, the domains are three dimensionally ordered. Within experimental error, the surface domain structure is identical to that of the bulk, indicating that the CDW propagates unaltered to the crystal surface.

An STM image was made of the surface of 1T-TaS_2 in the T phase at 225 K (Fig. 1A). The smallest visible periodic features in the figure are CDW maxima. Although surface defects obscure any obvious CDW domain structure, close inspection reveals long stripes running diagonally across the image from the upper left to the lower right. We interpret these stripes as CDW domains, where the bright stripes represent regions of enhanced CDW maxima, separated by dark lines of diminished CDW amplitude. From an analysis of six images from three samples we find that the average stripe width is 68 ± 5 Å and that the stripe boundary makes an angle of 28° ± 5° with the CDW translation vector direction, $\mathbf{T}_2$ (upper right corner of Fig. 1A). Here the CDW translation vectors, $\mathbf{T}_i$, are defined as

$$\mathbf{T}_i = 2\pi\, \mathbf{Q}_i \times z/\mathbf{Q}_1 \cdot \mathbf{Q}_2 \times z \qquad (1)$$

where z is a unit vector normal to the cleavage plane. The stripes appear to be at least as long as the largest scan (500 Å) we can obtain.

Unambiguous identification of CDW domain structure is possible by analysis of satellite structure in Fourier-transformed STM images (*7*) (Fig. 1B). The transform shows three pairs of strong peaks, labeled $\mathbf{Q}_1$, $\mathbf{Q}_2$, and $\mathbf{Q}_3$, which are the CDW fundamental peaks. Clear satellite peaks, labeled $\mathbf{Q}_{2sat}$ and $\mathbf{Q}_{3sat}$, occur near two of the three opposing pairs of CDW peaks. This fine satellite structure demonstrates a true domain modulation of the T phase CDW. The CDW wave vectors may be used to define a lattice, and the satellite peak positions may be expressed in terms of the CDW wave vectors. From an analysis of

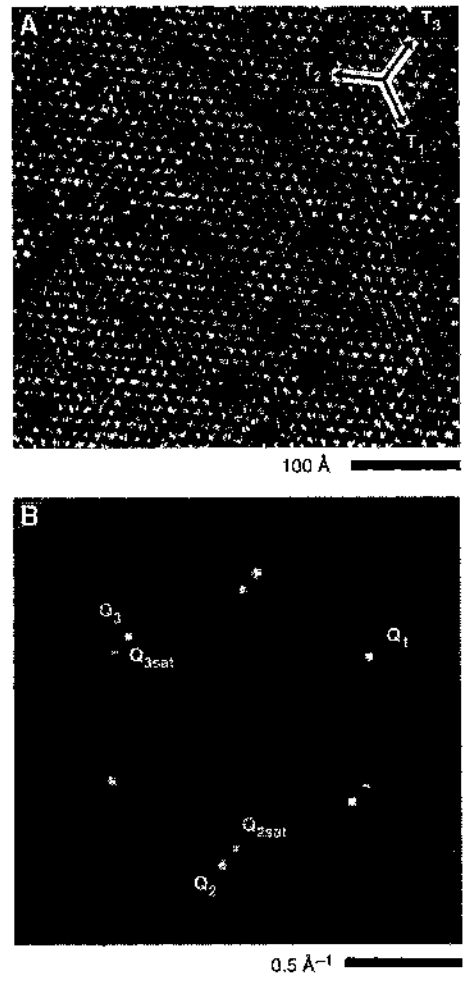

Fig. 1. (**A**) STM image of 1T-TaS_2 at $T = 225$ K in the T phase (constant height mode; tip bias, −20 mV; tunnel current, 5 nA). (**B**) Center of the Fourier transform of (A). CDW peaks are labeled $\mathbf{Q}_1$, $\mathbf{Q}_2$, and $\mathbf{Q}_3$, and satellite peaks are labeled $\mathbf{Q}_{2sat}$ and $\mathbf{Q}_{3sat}$.

Department of Physics, University of California, Berkeley, and Materials Sciences Division, Lawrence Berkeley Laboratory, Berkeley, CA 94720.

*To whom correspondence should be addressed.

the six Fourier-transformed STM data sets, we have determined the average satellite wave vectors and intensities relative to the CDW peak intensities. The uncertainties are ±0.02 for the $\mathbf{Q}_1$ and $\mathbf{Q}_2$ components of $\mathbf{Q}_{2sat}$ and $\mathbf{Q}_{3sat}$ (Table 1).

Our finding of a surface striped domain configuration is inconsistent with a previous x-ray diffraction study by Tanda and Sambongi (*10*) who, for the bulk material, determined a stretched honeycomb domain configuration with a width of 40 Å, a length of 250 Å, and an orientation of the long dimension of the stretched honeycomb at an angle of about 1° with respect to the CDW translation vector $\mathbf{T}_2$. In order to establish if this discrepancy reflects an intrinsic difference between the surface and bulk CDW structure in 1T-TaS_2, we undertook an x-ray diffraction study of the T phase CDW. We used a four-angle diffractometer to measure the CDW wave vectors and to search for fine satellite structure. A 1T-TaS_2 crystal (dimensions 0.2 by 0.2 by 0.05 mm) from a different batch from that used in our STM study was first cooled to the commensurate (C) phase at 150 K and held at that temperature for 1 hour before it was warmed to the T phase at 235 K. We measured CDW peaks positioned near the Bragg 110 peak. The position of the Bragg 110 peak was measured as well to provide a local reference. All peak parameters were determined by a "point and shoot" technique in which x-ray counts were sampled for a fixed time interval on a 9 by 9 by 9 three-dimensional grid centered on the approximately known peak positions. A three-dimensional Gaussian peak function was then fitted to the grid of points to extract peak coordinates, widths, and intensities.

The measured in-layer CDW wave vectors are shown as solid circles in Fig. 2. For the T phase CDW wave vectors, following the notation of Tanda and Sambongi (*10*), we find

$$\mathbf{Q}_1 = 0.231\ \mathbf{a}^* + 0.081\ \mathbf{b}^* + 0.437\ \mathbf{c}^* \quad (2a)$$

$$\mathbf{Q}_2 = 0.073\ \mathbf{a}^* - 0.321\ \mathbf{b}^* + 0.258\ \mathbf{c}^* \quad (2b)$$

$$\mathbf{Q}_3 = -0.305\ \mathbf{a}^* + 0.240\ \mathbf{b}^* + 0.305\ \mathbf{c}^* \quad (2c)$$

where the uncertainties are ±0.001 for the $\mathbf{a}^*$ and $\mathbf{b}^*$ components and ±0.002 for the $\mathbf{c}^*$ components.

In order to characterize the bulk domain configuration, we searched for fine satellite structure about each of the three CDW peaks. We found one near $\mathbf{Q}_2$ and one near $\mathbf{Q}_3$ (open circles in Fig. 2). Their positions are

$$\mathbf{Q}_{2sat} = 0.085\ \mathbf{a}^* - 0.279\ \mathbf{b}^* - 0.074\ \mathbf{c}^* \quad (3a)$$

$$\mathbf{Q}_{3sat} = -0.313\ \mathbf{a}^* + 0.199\ \mathbf{b}^* + 0.627\ \mathbf{c}^* \quad (3b)$$

The uncertainties on the $\mathbf{a}^*$ and $\mathbf{b}^*$ components are ±0.002 and the uncertainty on the $\mathbf{c}^*$ components is ±0.005. The observation of fine satellite structure by x-ray diffraction demonstrates that a periodic modulation of the CDW occurs in the bulk. The satellite wave vectors may be expressed in terms of the CDW wave vectors, as was done for the STM data, so that we can compare the two measurements directly. The results along with the x-ray–derived satellite intensities relative to the CDW intensities are included in Table 1; the agreement between the two sets of data is very good except for satellite intensities. The direct comparison of the intensities is complicated by x-ray structure factors which we have not attempted to include.

The bulk domain configuration extracted from the x-ray CDW and satellite peak positions and intensities is again striped, not a stretched honeycomb. A real-space reconstruction of the in-layer bulk domain configuration is obtained from the measured x-ray data (Fig. 3A). The gray scale indicates CDW electronic density. The image is formed from a superposition of a set of three sine waves using measured values of $\mathbf{Q}_1$, $\mathbf{Q}_2$, and $\mathbf{Q}_3$ to represent the CDW fundamental frequencies with a set of two sine waves using measured values of $\mathbf{Q}_{2sat}$ and $\mathbf{Q}_{3sat}$ and their relative intensities to represent the satellite frequencies. The reconstructed stripe width is 63 ± 3 Å, the length is greater than 600 Å, and the orientation of the long dimension of the stripe forms an angle of 24.5° ± 3.5° with the CDW translation vector direction, $\mathbf{T}_2$, indicated in the figure. In an electron diffraction study of the T phase, Withers and

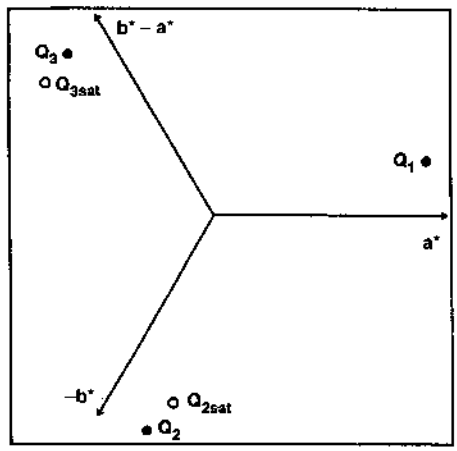

Fig. 2. In-layer CDW peaks (solid circles) and satellite peaks (open circles) at $T = 235$ K in the T phase obtained from x-ray diffraction.

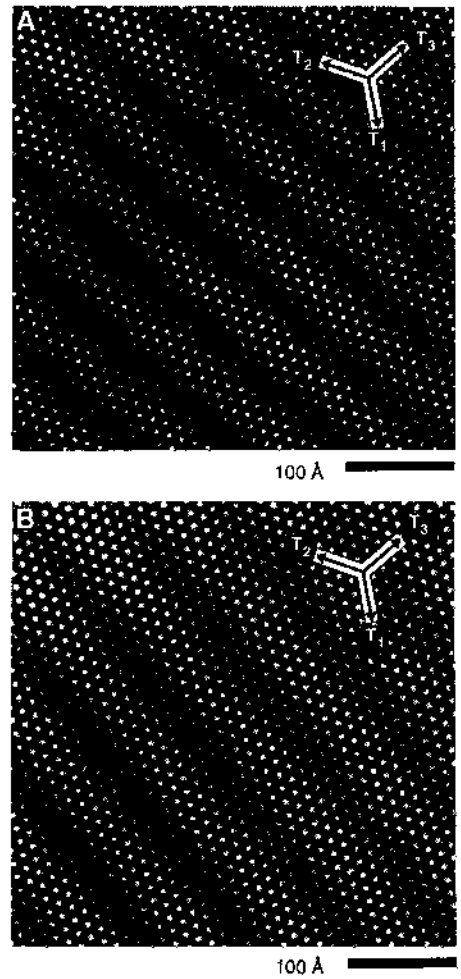

Fig. 3. Real-space reconstruction of the T phase in-layer CDW domain configuration (**A**) from the x-ray data and (**B**) from the measured Fourier components of the STM image (Fig. 1B).

Table 1. Comparison of the surface and bulk T phase CDW domain properties as measured by STM and x-ray diffraction, respectively, for 1T-TaS_2.

Property	STM (225 K), surface	X-ray (235 K), bulk
$\mathbf{Q}_{2sat}$	0.075 $\mathbf{Q}_1$ + 0.908 $\mathbf{Q}_2$	0.086 $\mathbf{Q}_1$ + 0.891 $\mathbf{Q}_2$
$\mathbf{Q}_{3sat}$	−1.072 $\mathbf{Q}_1$ − 0.908 $\mathbf{Q}_2$	−1.072 $\mathbf{Q}_1$ − 0.891 $\mathbf{Q}_2$
$\mathbf{Q}_{2sat}$ relative intensity	0.19	0.085
$\mathbf{Q}_{3sat}$ relative intensity	0.21	0.031
Stripe width	68 ± 5 Å	63 ± 3 Å
Stripe length	>500 Å	>600 Å
Stripe orientation	28° ± 5°	24.5° ± 3.5°

Steeds (12) identified "split peaks" (here called the CDW fundamental and satellite peaks), but they misinterpreted them as evidence that the T phase domain is not striped. In fact, the diffraction data of Withers and Steeds are consistent with the reconstruction in Fig. 3A.

The difference between the striped domain structure implied by our data and the stretched honeycomb structure obtained from the x-ray diffraction work of Tanda *et al.* (3, 10) may be traced to a slight disagreement in the measured CDW wave vectors. Our measurements differ from those of Tanda *et al.* by only a few thousands of a reciprocal lattice vector. The major result of the discrepancy is a rotation of the calculated domain structure by about 27° as well as an increase in the domain width and length. The domain configuration is exceedingly sensitive to the precise values of the CDW wave vectors. However, we can independently test the accuracy of our measured CDW wave vectors by calculating the expected positions of the satellites from the CDW wave vectors alone. The calculated and observed positions agree to within our experimental uncertainties.

The bulk domain configuration derived from our x-ray diffraction data is in close agreement with the surface domain configuration observed by STM. A real-space reconstruction of the surface in-layer domain configuration, from the Fourier components measured by STM, is shown in Fig. 3B. This image was generated with the same reconstruction method used for Fig. 3A. This reconstruction is equivalent to filtering the Fourier transform shown in Fig. 1B at the satellite and CDW peak frequencies and performing an inverse Fourier transformation. With the frequency components due to the defects (Fig. 1A) filtered out, the striped domain configuration is readily apparent in Fig. 3B. The good agreement between Fig. 3A and Fig. 3B is striking.

Because 1T-TaS_2 is both electronically and structurally a quasi–two-dimensional material, it may not seem too surprising that the surface and bulk CDW domain structures agree. In a material with weak interlayer coupling the absence of coupling from one side for a surface layer should not cause a serious perturbation to the CDW. However, x-ray diffraction studies (1, 10) have established a high degree of correlation of the CDW fundamental frequency across layers in the incommensurate (I), NC, and T phases. Therefore, interlayer coupling is significant, yet its absence from one side does not alter the CDW at the surface.

We expect significant interlayer coupling to correlate CDW domains across layers. Because the domain structure arises from the beating of the CDW frequencies with the satellite frequencies, the coherence of the domain structure along the c axis is determined by the coherence of both the CDW and the satellite frequencies. A lower bound for the coherence of each frequency may be obtained from the peak widths. From our Gaussian fits to the CDW and satellite peaks measured by x-ray diffraction, we obtain full width at half-maximum values, projected onto the c* axis, of about 0.035 c* for both cases. Roughly, this implies that domains are correlated across 20 layers in the T phase of 1T-TaS_2. The domain frequency along the c axis is simply the difference, about c*/3, between the c* components of a CDW wave vector and its satellite. Thus, the striped domain configuration exhibits a three-layer stacking.

REFERENCES AND NOTES

1. C. B. Scruby, P. M. Williams, G. S. Parry, *Philos. Mag.* 31, 255 (1975).
2. S. C. Bayliss, A. M. Ghorayeb, D. R. P. Guy, *J. Phys. C* 17, L533 (1984).
3. S. Tanda, T. Sambongi, T. Tani, S. Tanaka, *J. Phys. Soc. Jpn.* 53, 476 (1984).
4. K. Nakanishi, H. Takatera, Y. Yamada, H. Shiba, *ibid.* 43, 1509 (1977).
5. K. Nakanishi and H. Shiba, *ibid.*, p. 1893.
6. X. L. Wu and C. M. Lieber, *Science* 243, 1703 (1989).
7. B. Burk, R. E. Thomson, A. Zettl, J. Clarke, *Phys. Rev. Lett.* 66, 3040 (1991).
8. R. V. Coleman, W. W. McNairy, C. G. Slough, *Phys. Rev. B* 45, 1428 (1992).
9. K. Nakanishi and H. Shiba, *J. Phys. Soc. Jpn.* 53, 1103 (1984).
10. S. Tanda and T. Sambongi, *Synth. Metals* 11, 85 (1985).
11. R. E. Thomson *et al.*, *Phys. Rev. B* 38, 10734 (1988).
12. R. L. Withers and J. W. Steeds, *J. Phys. C* 20, 4019 (1987).

13. We thank F. Hollander for valuable assistance with x-ray diffraction. This work was supported by NSF grant DMR-90-17254 (B.B. and A.Z.), and by the Director, Office of Energy Research, Office of Basic Energy Science, Materials Science Division of the U.S. Department of Energy, under contract DE-AC03-76F00098 (R.E.T. and J.C.).

11 March 1992; accepted 26 May 1992

Direct Electrochemical Measurements Inside a 2000 Angstrom Thick Polymer Film by Scanning Electrochemical Microscopy

Michael V. Mirkin, Fu-Ren F. Fan, Allen J. Bard*

An extremely small, conically shaped Pt microelectrode tip (with a radius of 30 nanometers) and the precise positioning capabilities of the scanning electrochemical microscope were used to penetrate a thin (200 nanometers) polymer film and obtain directly the standard potential and kinetic parameters of an electrode reaction within the film. The thickness of the film was determined while it was immersed in and swollen by an electrolyte solution. The film studied was the perfluorosulfonate Nafion containing $Os(bpy)_3^{2+}$ (bpy, 2,2′-bipyridine) cast on an indium tin oxide surface. The steady-state response at the ultramicroelectrode allowed direct determination of the rate constant for heterogeneous electron transfer k° and the diffusion coefficient D without complications caused by transport in the liquid phase, charge exchange at the liquid-polymer interface, and resistive drop.

The advent of ultramicroelectrodes (1) has encouraged attempts at electrochemical studies in very small structures, for example, within single biological cells (2) or tiny drops of solution (3). Such probes are also useful for studying electrochemical processes in thin films. The electrochemistry of films of ionically conducting polymers, such as Nafion, that contain redox species has been studied extensively (4, 5), but questions still remain about the distribution of species and the rates of mass transfer and electron transfer (ET) within the film. The typical experimental approach in such studies involves formation of a polymer film of nanometer to micrometer thickness by spin or drop coating followed by electrochemical studies of the film-substrate region as an electrode in contact with a solution containing one or more redox active species. Alternative structures that have been used include electroactive polymers with metal-sandwich and interdigitated array structures coated on microelectrodes (6). The current, determined by the ET rate at the substrate-film interface, can be governed by a number of processes, including diffusion in solution, charge transfer or extraction at the film-solution interface, mass transfer and ET reactions within the film, movement of co-ions, and heterogeneous ET processes at the film-substrate interface. The existence of all of these processes, as well as the added problem of film resistivity, greatly complicates the determination of kinetic parameters (such as k° and D) as functions of film loading with electroactive species and solu-

Department of Chemistry and Biochemistry, University of Texas at Austin, Austin, TX 78712.